

Effects of Rotors on UUV Trajectory Planning Via the Virtual Potentials Method

Matko Barisic^{#1}, Zoran Vukic^{#2}
Nikola Miskovic^{#3}

*[#]Laboratory for Underwater Systems and Technologies, University of Zagreb,
Faculty of Electrical Engineering and Computing, Unska 3, HR-10000 Zagreb*

¹matko.barisic@fer.hr

²zoran.vukic@fer.hr

³nikola.miskovic@fer.hr

Abstract— A method for the trajectory planning of coordinated groups of UUVs, developed in authors' previous work is extended. The key points within the design patterns that must be used to implement the method in code are stressed. Rotors, vectorized quantities which introduce directionality, and thereby cause divergence from local minima, are introduced into the virtual potential algorithm. This development is compared with the strategy for local minima avoidance previously employed by the authors. Testing is done by simulation and comparison of simulated system responses.

I. INTRODUCTION

The authors have, in previous work [1] – [4], developed and simulated a framework for online trajectory replanning for UUVs. The framework has been developed and is being extended and advanced with the intention of coordinated control of UUV schools. One of the key design features of the system, primarily motivated by the nature of the underwater environment, and explored in [5] and [6] is that communication is eschewed in favor of sonar-based sensing. The design methodology is the incorporation of the trajectory planner into a hierarchical distributed total control solution, although other strategies (such as the one described by the authors of [7]) have been studied by the authors. The framework searches for an optimal trajectory by calculating a neighborhood virtual potentials map. The virtual potentials approach was originally motivated by insight into the works of authors of [8 – 10]. This map is influenced by obstacles, goal-points of the Itinerary, individual agents, and agents groups - formations. The authors have dedicated a portion of their previous work to the avoidance of local minima based on the automated insertion of “ghost goal points”, according to [3] and [4].

The findings of previous research, together with a clearer systematization of the command signals generated by the framework are presented in Section 2. By further developing equations adopted in authors' previous work, more space is dedicated to comments of the framework's functionality optimality, robustness and resilience within the hard-real time implementation. The framework's intended prototype application is within a future micro-AUV system, based on the commercially available VideoRay Pro ROV, and realized

as its autonomization – [10]. Section 3 lays out the theory, reasoning and numerical mathematics behind rotors, a scheme of local minima avoidance with better qualities than the existing one, utilizing “ghost goal points”. Section 4 presents evidence to the latter claims by comparing simulation results for both methods. Section 5 concludes the paper.

II. THE FRAMEWORK

A. Existing framework capabilities

The object of research in this paper is an algorithm for the on-line re-planning of coordinated trajectories assuring formational navigation of UUVs. Clutter and obstructions in the UUVs' theater of operations are successfully circumnavigated. The prerequisite exploratory and system analysis work (modeling of the dynamics) on an autonomized micro-ROV platform, operated by the authors in related investigative work, has been described in [11 – 13].

The trajectory re-planning algorithm functions in 2D since depth actuation for a group of UUVs carrying out a surveying mission is generally handled by a separate and independent control loop relying on altimetry (distance from the bottom). This virtual potentials framework coordinates and re-plans UUVs' trajectories in the surge-sway plane. Speaking from a “block diagram” viewpoint of the UUV's control hierarchy, the frameworks outputs are a group of six commands. These allow the course and forward speed of the UUV to be effectively controlled along the planned trajectory by decoupled LTI controllers for the surge and yaw.

Its inputs are twofold:

- a list of parameters for each obstacle detected by a sonar or camera.

In a real, embedded system, these parameters are calculated by some feature-extracting scheme working in hard-real-time on the raw sensor data streaming from the sonar.

- A list of parameters of one by one out of a set of goal-points called the Itinerary.

The goal-point potential distribution function (PDF) is based on the 2d Gauss curve, as exemplified by figure 1. Obstacles, on the other hand, are classified as being of one of the types from the collection including the following: orthogonal (figure 2), elliptic (figure 3), circular (figure 4) or triangular (figure 5) class.

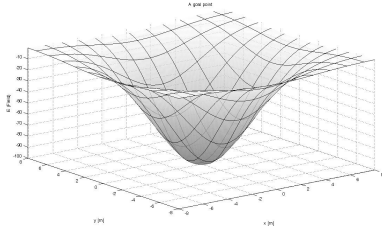


Fig. 1 The goal-point PDF

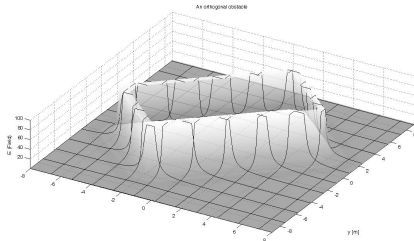


Fig. 2 The orthogonal PDF

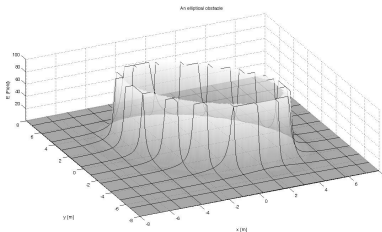


Fig. 3 The elliptic PDF

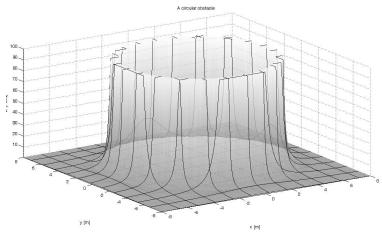


Fig. 4 The circular PDF

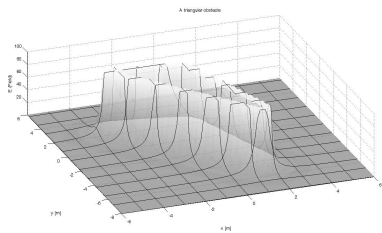


Fig. 5 The triangular PDF

Detailed mathematical definitions of the potential distribution functions can be found in [1] – [4]. Basically, the repulsiveness of an obstacle is defined by the slope of its potential contribution E_{obst} , which is positive and monotonously decreases with the distance from the obstacle. The exact calculation of the r metric is class-dependent. Therefore, without quoting specific formulae for r , the following is the prototype of the E_{obst} potential distribution function:

$$E_{obst}(\vec{p}) = \exp\left(-A^+ / r(\vec{p}, \vec{p}_{obst})\right) - 1 \quad (1)$$

Where r is the \mathbb{R}^2 distance between point p of interest and the obstacle's closest boundary (a vertex, face or continuous arc, depending on the class of an obstacle). Subsequently, the calculation of r ranges from the trivial (circular obstacles) to the involved (triangular or elliptic obstacles). Details are available in [3] and [4].

The interaction between coordinating UUVs is effected by supposing that they exhibit potential influences on one another, such that it has both positive and negative areas. An indefinitely repulsive boundary around a critical vicinity of another agent (“agent” is used interchangeably with “UUV”) is guaranteed, preventing collision. However, an additional feature of such a superposition of influences is the occurrence of local minima depending on the geometry of the desired formation. It is intended that these geometries be chosen from complete tilings of an indefinite 2d surface (equilateral triangles, squares, regular hexagons). An example (for a regular hexagon) is shown in figure 6.

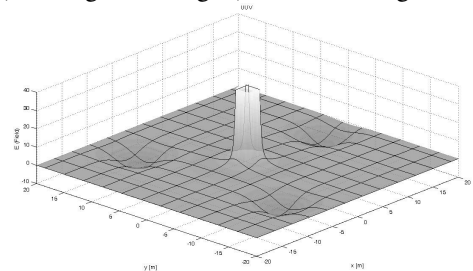


Fig. 6 The agent PDF

B. Command signals

The gradient of the potential, from which both the direction and the amount of control action are arrived at, is numerically approximated by a radial sampling of the n_ϵ points of the potential field spaced equidistantly on an ϵ -radius circle around the UUV. The sampling is therefore parameterized by a pair (n_ϵ, ϵ) . This produces a finitely good numerical approximation of the true gradient, since the direction is quantized in $2\pi n_\epsilon$ steps, as in figure 7.

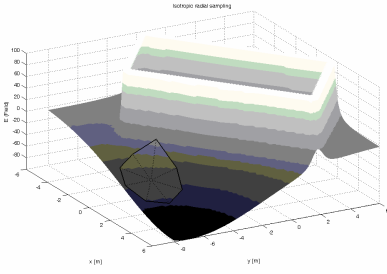


Figure 7: Radial sampling of the potential field

The numerical approximation of the gradient of the sum potential field ∇E , is called the *propellant force*, F . Depending on the scheme of control employed aboard a UUV, and in the interest of generality, this quantity can be used in a different manner than the approach described herein, e.g. more directly in thrust-vector-space, if such is known, modeled and applicable to a particular UUV's control.

F is further modified by the dissipative action of a *virtual friction force* $F_{\text{vfric}}(k)$. This modification needs to be included in order to guarantee stability of the planned trajectory, by virtue of turning a conservative system into a dissipative one. The stability-guarantee and the repercussion of this modification are researched and described in [1] – [4]. The norm of F is subject to the upper bound of F_{max} , a UUV-dependent technical parameter.

For purposes of clarity of following mathematics, a quantity called the *reference acceleration vector* $a(k)$ is introduced, and figured as equal to F by assuming unit “virtual mass” of the point-model agent.

The acceleration vector is numerically integrated (bilinear formula; [13]) into the *reference velocity vector* $v(k)$. This acceleration is then decomposed into components co-linearly and perpendicularly to $v_m(k)$, the actual, measured velocity at instant k :

$$\bar{a}(k) = \langle \bar{a}(k), \bar{e}_1 \rangle \cdot \bar{e}_1 + \langle \bar{a}(k), \bar{e}_2 \rangle \cdot \bar{e}_2 \quad (2)$$

Wherein e_1 and e_2 are an orthonormal base in \mathbb{R}^2 defined by

$$\langle \bar{v}_m(k), \bar{e}_1 \rangle = 1 \quad (3)$$

$$\langle \bar{v}_m(k), \bar{e}_2 \rangle = 0; e_1 = \|\bar{e}_1\| = 1 \quad (4)$$

The co-linear coefficient is stored as the *surge acceleration command* $a_c(k)$.

$$a_c(k) = \langle \bar{a}(k), \bar{e}_1 \rangle \quad (5)$$

The norm and angle of the reference velocity $v(k)$ are stored as the *surge speed command*– $v_c(k)$ and the *yaw command* – $\phi_c(k)$, respectively. The surge speed command has an upper bound of v_{max} , a UUV-dependent technical parameter.

$$v_c(k) = \lceil \|\bar{v}(k)\| \rceil^{v_{\text{max}}} \quad (6)$$

$$\phi_c(k) = \arg(\bar{v}(k)) = \text{atan2}(\bar{v}(k)) \quad (7)$$

The course command is differentiated (by the use of the system sample time T), $(\phi_c(k) - \phi_c(k-1))/T$, to get the *rate-of-yaw command* $\omega_c(k)$:

$$\omega_c(k) = [\phi_c(k) - \phi_c(k-1)] / T \quad (8)$$

The radius-of-turn $r_T(k)$ is calculated from (6) and (8):

$$r_T(k) = \omega_c(k) / v_c(k) \quad (9)$$

The radius-of-turn is used to compute and store the *angular acceleration command* $a_c(k)$:

$$\alpha_c(k) = \frac{r(k) \cdot a_c(k) - v_c(k) \cdot \{[r(k) - r(k-1)] / T\}}{r^2(k)} \quad (10)$$

Equations (5, 6, 8 and 10) provide the derivative and proportional commands for a pair of decoupled rate-of-yaw and surge speed controllers at the level “below” the trajectory planner. To appreciate the subdivision into hierarchical “levels” of the UUV's control system used systematically throughout this paper, the reader is invited to refer to [1].

The difference between the $\phi_c(k)$ and the measured course $\phi_m(k)$ can be used to as the *integral channel of the course controller*, I_{course} (possibly modified by an integral time constant of the course-control loop).

The ideal (commanded) position $p_{UUV(c)}$ is calculated by integrating $v(k)$. The norm of the difference-vector between $p_{UUV(c)}$ and the measured position, $p_{UUV(m)}$, Δp , is calculated:

$$I_{\text{surge}} = \Delta p = \|\bar{p}_{UUV(c)} - \bar{p}_{UUV(m)}\| \quad (11)$$

This constitutes the *integral channel signal of the surge-speed controller*, I_{surge} (possibly modified by an integral time constant of the surge-control loop).

The structure and architecture of lower levels of the UUV's control system to which the usage of this framework as a reference generator is covered in more detail in [10] – [11]. However, the presented framework is in this respect modular since any or all of these commands can be included or excluded by some custom lower level controller. Additional or transformed command signals can easily be calculated on-line from the running signals (e.g., the radius-of-turn can be used directly, as well as other metrics to run some sort of an optimal control loop).

III. THE ROTOR POTENTIALS

The authors have, in previous research, made use of an approach to local minima avoidance using the introduction of “ghost goal-points”. Although proven effective – [3] and [4], this approach suffers from a number of drawbacks.

A. Theoretical

A.1. Regardless of the choice of parameters used to initiate the “ghost goal point” calculation procedure, the “detour

leg” introduced in this respect into the school’s itinerary is *in general never optimal*.

Functional (Implementation-related)

B.1. The introduction of “ghost goal points” burdens the onboard memory. This approach requires a second stack that will contain the “ghost Itinerary”. The size of this stack has a non-deterministic upper bound, since its “depth” (number of possible “detours-of-detours...”) is completely arbitrary and dependent upon the expected level and geometrical setup of clutter in the theater of operation.

B.2. Alternatively, “ghost” goal points can be “bundled together” with the actual goal points in the one and the same Itinerary. However, in addition to being non-transparent and difficult to debug, this does not help. The memory burden arises in this variant in the form of a heap of additional pointers into the Itinerary stack which sort out the “ghost” goal points and the actual ones. Also a dynamically allocated array of counters of detour legs (since it is possible to have a situation producing a “detour-of-a-detour...”) is required.

B.3. The introduction of either of the approaches also requires changes to the structure and functionality of the programmed methods. The changes encumber the CPU and degrade hard-real-time performance.

As an alternative, the local minima avoidance problem was approached from a different perspective. The authors have modified the existing potential distribution functions. A rotor component is added to the stator PDF description of obstacles.

The effect of the rotor on an ordinarily isotropic potential map introduces an anisotropism: a directionalized “sliding slope” of potential. This is always oriented so to “shove” the agent around an obstacle, as demonstrated in figure 8. The “shoving” action is irrespective of the relative positions of the agent and the obstacle, since the slope itself rotates about the barycenter of the obstacle.

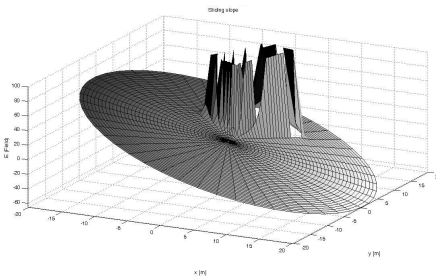


Figure 8: “Sliding slope” effect of a rotor

The brief on the form of the stator part of every obstacle class’s PDF has been given in Section 1. In marked contrast to the stator part’s dependence solely on the non-directional metric r , the rotor PDF is a vector. Its direction depends on the agent-relative geometry of the theater of operations. Specifically, the rotor’s direction depends the relation between the agent-relative positions of the obstacle’s

barycenter and the goal-point. This dependence of the rotor’s direction θ on agent-relative geometry is given by equations (13 – 16). The consequences of these equations are schematically presented in figure 11.

In the following equations, $\mathbf{R}(\cdot)$ is the operation of rotation (left-multiplying a 2×1 2d vector with a rotation matrix), and γ is the symbol used for the relative azimuth (bearing). Superscripts index the reference point and the subscripts the point which azimuth is determined. Indices have the following meanings: *obst* – obstacle (barycenter); *GP* – goal point (a point); *UUV* – the agent under consideration.

$$\gamma_{obst}^{GP} = \arg(\vec{p}_{obst} - \vec{p}_{GP}) = \text{atan2}(\vec{p}_{obst} - \vec{p}_{GP}) \quad (13)$$

$$\gamma_{UUV}^{GP} = \arg(\vec{p}_{UUV} - \vec{p}_{GP}) = \text{atan2}(\vec{p}_{UUV} - \vec{p}_{GP}) \quad (14)$$

$$d = \begin{cases} 0.5\text{sgn}(\gamma_{obst}^{GP} - \gamma_{UUV}^{GP}) - 0.5; & \text{sgn}(\gamma_{obst}^{GP} - \gamma_{UUV}^{GP}) \neq 0 \\ -1 & \gamma_{obst}^{GP} = \gamma_{UUV}^{GP} \end{cases} \quad (15)$$

$$\theta = \mathbf{R}(d\pi / 2) \cdot \delta_{UUV}^{obst} \quad (16)$$

δ_{UUV}^{obst} is the *boundary normal* angle, directed from the UUV towards the obstacle. However, it is *not generally* the azimuth of the obstacle’s barycenter relative to the UUV (except in the trivial case of a circular obstacle). The boundary normal is an inwards facing vector normal to the boundary (vertex, face or continuous arc) of the obstacle closest to the UUV, as displayed in figure 9.

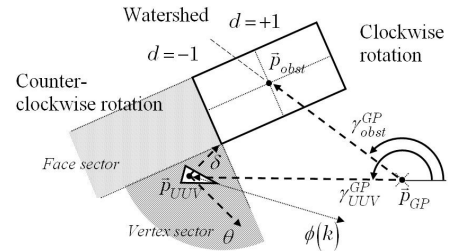


Figure 9: Relationships between the agent-relative geometry and θ

In addition to coding equations (13 – 16) into the framework, a cut-off metric was introduced. This cut-off was introduced for reasons of computational sparseness so that rotor effects of obstacles far from the agent are not present in the calculation procedure. An example of this rotor is given, for an orthogonal class of obstacles, in figure 10.

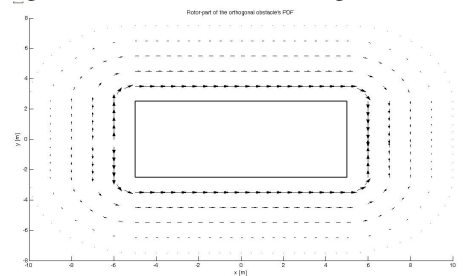


Figure 10: The rotor part of an orthogonal obstacle class PDF

IV. SIMULATION

A comparative simulation of online trajectory planning was performed. In the simulated “sanity test” for the proposed hypothesis, both the “ghost goal point” – GGP, and the rotor approach – ROT, are tested within an unrealistically cluttered theater of operation for the case of a single UUV (for clarity of graphical results). Figures 11 – 14 display the static potential map of the theater of operations, the ROT-method trajectory and the GGP-method trajectory and the comparison of the speed commands starting with the period of approach to the (first) local minimum.

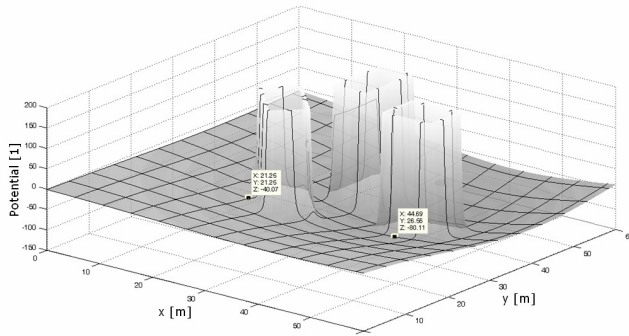


Figure 11: Static virtual potential map of the theatre of operations

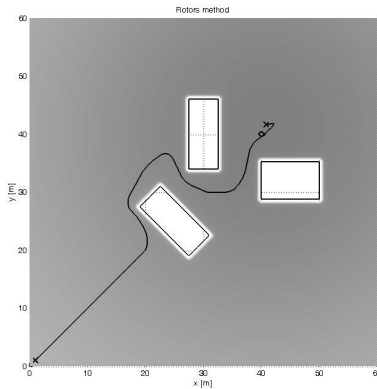


Figure 12: Trajectories planned by the ROT method

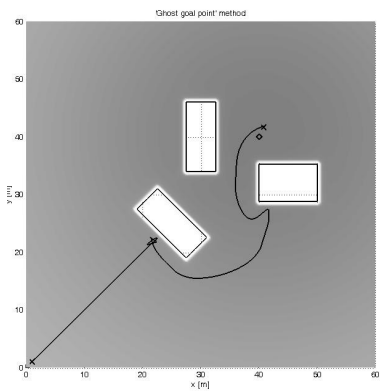


Figure 13: Trajectories planned by the GGP method

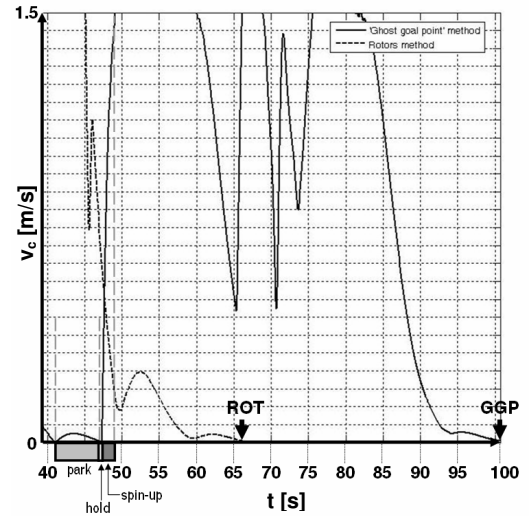


Figure 14: Comparison of surge speed command signals for both methods

As is visible from the results of the experiment, the “ghost goal point” method produces suboptimal trajectories. The length of the path traversed, and the time of termination are both inferior to the trajectory produced by the rotor method.

The difference between the times of both variants’ execution in the first experiment is 400 sampling intervals in favor of the rotor-method. For a UUV operating at the sample time of 0.1s, this translates to 40s. A fair comparison of the two methods needs additionally leverage in favor of the “ghost goal point method”. Namely, the latter method can be further optimized by a tuning procedure for the parameters needed to calculate the “ghost goal point”. Also an approach to the “ghost goal points” is defined by the n_{ap} sampling periods during which the agent is effectively at the “ghost goal point” (before the actual goal point is reintroduced into the trajectory re-planning). During this period the “ghost goal point” method is functionally inactive. This hiatus occurs once per detour leg. Even if this leverage is applied in favor of the “ghost goal point” method, the discrepancies in the times of execution are unequivocally in favor of the rotor method.

The shape and the regions of the theater of operation traversed by the rotor-method are much more suited to the mission.

V. CONCLUSIONS

A. Overview

In conclusion, the framework presented in author’s previous work was improved by the inclusion of the rotor component to the obstacles’ PDF. This approach is functionally transparent and modular. Additionally, it was tested in simulation against an existing local minima avoidance scheme – one using “ghost goal points”. The analysis of the simulation, performed as a sanity test, it was shown to be better suited to the task of local minima avoidance than the previously adopted scheme.

This framework is intended as a “middle” level of a hierarchical (cf. [1]) intelligent control system for

coordinated UUVs under development in the authors' laboratory.

The position of this framework within a hierarchical tier is above (and therefore dictating the servo commands or set-points) the level of immediate UUV drive controllers. In a "top-to-bottom" view, the framework serves appropriate command signals for lower-level controllers which control the immediate current loops of the UUV's drives.

Additionally, the key point of this framework in a "bottom-to-top" approach to the hierarchy is that it *abstracts* the trajectory planning. In that way, the command parameters of this trajectory planner can easily be accessed and changed by semantic programming. This is a necessity for its interactivity with the higher level of the control hierarchy, which encodes intelligent functions like fault-tolerance, mission scenario adaptation, and automated reasoning about the success of the mission.

B. Future research

Future research will be directed in the following topics:

- 1) Eliminating "parking creep" and "smoothing" the dynamics of the formation – [3, 4].
- 2) Exploring how the holonomy supposition can be alleviated, possibly by including a diffeomorphism alike to the one explored in [14]. This will expand the envelope of constraints to the performance and design of lower level controllers by eliminating unfeasible ordered pairs of yaw- and surge-commands.
- 3) Estimation of stationary stochastic disturbances in the theater of operations (currents, wave motion, drift etc.) from the trends exhibited in the measurement signals and the dynamic regimes of the difference in the commands and measurements.

ACKNOWLEDGMENT

This research is supported by The "RoboMarSec - Underwater robotics in sub-sea protection and maritime security" project, no. 036-0362975-2999, of the Ministry of Science, Education and Sports of the Republic of Croatia.

This research is also supported by financial and infrastructural resources of the "Center for Underwater Systems and Technologies" (CUST), a Croatian-based non-for-profit organization of maritime engineering and research professionals.

REFERENCES

Barisic, M., Z. Vukic and N. Miskovic: "Design of a coordinated control system for marine vehicles". In: *Proceedings of the 6th IFAC Conference on Manoeuvring and Control of Marine Craft* (Pascoal, A.), on CD. Instituto Superior Technico, Lisbon, Portugal, October 2006.

Barisic, M., Z. Vukic and N. Miskovic: "Kinematic Simulative Analysis of Virtual Potential Field Method for AUV Trajectory Planning". In: *Proceedings of the 15th Mediterranean Conference on*

Control and Automation, (Valavanis K. and Kovacic, Z.), on CD. Mediterranean Control Association, Athens, Greece, June 2007.

Barisic, M., Z. Vukic and N. Miskovic: "A Kinematic Virtual Potentials Trajectory Planner For AUV-s. In: *Proceedings of the 6th IFAC Symposium on Intelligent and Autonomous Vehicles*, (Devy, M.), on CD. Laboratoire d'Architecture et d'Analyse des Systèmes, Toulouse, France, September 2007.

Barisic, M., Z. Vukic, N. Miskovic and B. Tovornik: "AUV Formations Achieved By Virtual Potentials Trajectory Planning In A Simulated Environment". In: *Proceedings of the 7th IFAC Conference on Control Applications in Marine Systems*, (Vukic, Z. and Longhi, S.), on CD. Center for Underwater Systems and Technologies, Zagreb, Croatia, September 2007.

Beard, R. W. and McLain, T. W.: "Multiple UAV Cooperative Search under Collision Avoidance and Limited Range Communication Constraints". In: *Proceedings of the 42nd IEEE Conference on Decision and Control*, pp. 25-30, year 2003.

Bellingham, J. S. et al.: "Cooperative Path Planning for Multiple UAVs in Dynamic and Uncertain Environments". In: *Proceedings of the 41st IEEE Conference on Decision and Control*, pp. 2816-2822, year 2002.

Kalantar, S. and Zimmer, U.: "Motion planning for small formations of autonomous vehicles navigating on gradient fields". In: *Proceedings of The International Symposium on Underwater Technology, UT 2007 - International Workshop on Scientific Use of Submarine Cables and Related Technologies 2007* (Ura, T., Wernli R. and Kasahara J.), pp 512-519. Institute of Industrial Science, University of Tokyo, Tokyo, Japan, 2005.

Fax, J. A. and Murray, R. M.: "Information Flow and Cooperative Control of Vehicle Formations". In: *IEEE Transactions on Automatic Control*, vol. 49, issue 9, pp. 1465-1476, year 2004.

Moreau, L., Bachmeyer, R. and Leonard, N. E.: "Coordinated Gradient Descent: A Case Study of Lagrangian Dynamics With Projected Gradient Information". In: *Proceedings of the 2nd IFAC Workshop on Lagrangian and Hamiltonian Methods for Nonlinear Control*, Universidad de Sevilla, Sevilla, Spain, 2003.

Sepulchre, R., Paley, D. and Leonard, N. E.: "Graph Laplacian and Lyapunov Design of Collective Planar Motions. In: *Proceedings of the International Symposium on Nonlinear Theory and Its Application* (Oishi, S. and Vandewalle, J.), The Institute of Electronics, Information and Communication Engineers, Tokyo, Japan, 2005.

Stipanov, M., N. Miskovic, Z. Vukic and M. Barisic: "ROV Autonomization - Yaw Identification and Automarine Module Architecture". In: *Proceedings of the 7th IFAC Conference on Control Applications in Marine Systems*, (Vukic, Z. and Longhi, S.), on CD. Center for Underwater Systems and Technologies, Zagreb, Croatia, June 2007.

Miskovic, N., Z. Vukic, and M. Barisic: "Transfer Function Identification by Using Self-Oscillations". In: *Proceedings of the 15th Mediterranean Conference on Control and Automation*, (Valavanis K. and Kovacic, Z.), on CD. Mediterranean Control Association, Athens, Greece, June 2007.

Miskovic, N., Z. Vukic, M. Barisic and P. P. Soucacos (2007). AUV Identification by Use of Self-Oscillations. In: *Proceedings of the 7th IFAC Conference on Control Applications in Marine Systems*, (Vukic, Z. and Longhi, S.), on CD. Center for Underwater Systems and Technologies, Zagreb, Croatia, September 2007.

Vukic, Z. and Lj. Kuljaca: "Automatic Control: Analysis of linear systems", (Ed.: Neven Lihtar) Kigen, Zagreb, Croatia, 2004.

Fadenza, P. V. and P. U. Lima: "Non-holonomic robot formation with obstacle compliant geometry". In: *Proceedings of the 6th IFAC Symposium on Intelligent and Autonomous Vehicles*, (Devy, M.), on CD. Laboratoire d'Architecture et d'Analyse des Systèmes, Toulouse, France, September 2007.